A Correction for the Errors in Ship Reports of Light Winds

BARRY B. HINTON AND DONALD P. WYLIE

Space Science and Engineering Center, University of Wisconsin-Madison, Madison, WI 53706

(Manuscript received 10 April 1984, in final form 14 February 1985)

ABSTRACT

The errors in ship wind reports of light winds tend to significantly bias their mean. This occurs because wind speed is a scalar quantity that is constrained to zero or positive values. Therefore, observations tend to overestimate the light winds because of the one-sided distribution of errors, but the bias disappears under stronger winds. A method for removing this bias from ship data is presented. In particular, the method is applied to interpreting the ratios of wind speeds observed by ships to those obtained from tracking low level clouds. Corrected ratios allow low cloud speeds to serve as proxy data for surface based observations.

1. Introduction

In the absence of adequate surface data, investigators sometimes infer winds over the oceans from proxy data. Two data types often used are speeds of low level clouds tracked in satellite images and, when an adequately defined pressure field is available, geostrophic winds. These are then compared to ship reports to infer the accuracy of the proxy data. The speed ratios—surface speed over cloud speed or the surface speed over geostrophic speed—are usually calculated as one step in the transformation of winds from a higher level to a lower one. In this brief paper, we discuss certain errors that can systematically distort the empirical determination of these ratios, and how they may be corrected.

2. Correction of wind speed reported by ships

Well over half, possibly 80% or more, of winds reported by cooperative ships are based on sea state observations by means of a Beaufort scale of wind force. Some of the history surrounding this scale and various wind speed equivalents to 1970 can be found in WMO (1970). In general, the "steps" in the scale are ~ 2 m s^{-1} (low speeds) to ~ 3 m s^{-1} (high speeds). In archived data, the reports are usually given as integral values by knots. This quantification can lead to errors in the reports which need to be removed from the data.

The wind speed U_t is measured by a reference observing system. Ideally, it would be the true speed, but in practice it will be a preferred set of measurements. Our objective is to correct a second set of observed wind speeds (U_0) to achieve agreement with U_t. In this context we may think of $U_0 - U_t = E$ as an "error" of individual observations. The probability distribution, $f(E)$, has two complicating features. First, if only discrete values are recorded, as is the case for ship data, then for a given value of U_t, $f(E)$ will be discontinuous. But more important, speed is constrained to be zero or positive. Consequently, if $U_t = 0$, only positive errors are possible. Even if $U_t > 0$ but is smaller than a typical value of E, the positive errors will outweigh the negative. On the other hand, when U_t is somewhat greater than a typical value of E, the frequency distribution, $f(E)$, should approximate a Gaussian distribution with a mean of zero. After "blunder point" editing, the resulting error distribution for actual data is Gaussian-like outside of light wind areas. If σ^2 is the variance, we can tentatively write the probability distribution, $f(e)$, of the normalized error, $e = (U_0 - U_t)/\sigma$, as a truncated Gaussian function.

$$f(e) = \begin{cases} (2\pi)^{1/2} \exp(-e^2/2) & \text{for} \quad e \geq U_t/\sigma \\ 0 & \text{for} \quad e < -U_t/\sigma. \end{cases} \tag{1}$$

The conditions on e in (1) are derived from the fact that no observation is accepted with U_0 less than zero. The definition of e implies $e + U_t/\sigma \geq 0$ (since $e + U_t/\sigma = U_0/\sigma$) in order that $f(e)$ may be nonzero. In order to make the integral of (1) over its range equal to unity, as is required of any probability distribution, we must divide by (2).

$$\int_{-\infty}^{+\infty} f(e)de = \int_{-U_t/\sigma}^{+\infty} (2\pi)^{-1/2} \exp(-e^2/2)de. \tag{2}$$

Thus, the correctly normalized error distribution, $g(e)$ is found in (3).

$$g[(U_0 - U_t)/\sigma] = f[(U_0 - U_t)/\sigma] \Big/ \int_{-U_t/\sigma}^{+\infty} f(e)de. \tag{3}$$

Now we can calculate the mean value of the error as

$$\bar{e} = \int_{-\infty}^{+\infty} eg(e)de = \int_{-U_t/\sigma}^{+\infty} eg(e)de. \tag{4}$$

As expected, $\bar{e}$ is not zero. Table 1 displays a few values of $\bar{e}$ (columns 2 and 5) as a function of U_t/σ (columns 1 and 4). Using these, and the definition of e, one can calculate the expected value of the mean of the observed speed divided by σ (shown in columns 3 and 6) from (5);

$$U_t/\sigma + \bar{e} = \bar{U}_0/\sigma. \quad (5)$$

In several investigations we have compared wind estimates from neighboring ships (Wylie and Hinton, 1982). These studies consistently suggest that σ is the order of 2.5–3.0 m s^{-1}, as one might suppose from the step size of the Beaufort scale.

To test our predicted relation between $\bar{U}_0$ and U_t, we compared ship wind speed estimates with measurements of three nearby NOAA data buoys in the Gulf of Mexico. We believed the buoy observations to be more accurate because of the subjectivity of the Beaufort scale and difficulty of correctly interpreting anemometer readings from a moving ship. Thus, we let buoy data play the role of U_t. The results are shown in Fig. 1 by the Xs. Note that under light winds the mean of the ship reports is higher than the buoy reports. Estimates of $\bar{U}_0$ as a function of U_t from Table 1 for the cases σ = 2.5 and 3.0 m s^{-1} are shown in Fig. 1. These estimates confirm that $\bar{U}_0$ could be "corrected" to be more nearly in agreement with the U_t using an approximate value of 2.5–3 m s^{-1} for σ. By a trivial manipulation of (5), we obtain the relationship,

$$\bar{U}_t = \bar{U}_0 - \sigma\bar{e}. \quad (6)$$

This says that if the mean of a large set of observations is modified by subtracting $\sigma\bar{e}$, we can replicate the mean of the corresponding U_t from the reference data set. Residual errors may still arise if the sample size is small so that the sample means do not match the means of the total population, if the probability distribution is not well approximated by (1)–(4), or if σ is chosen incorrectly. However, if reasonable approximations are available for these, the right side of (6) will usually be much closer to $\bar{U}_t$ than the unmodified $\bar{U}_0$ would be.

TABLE 1. Mean values of speed error and expected value of mean speed. For U_t/σ entries greater than 2.5, $\bar{e}$ differs negligibly from 0 so that $U_t/\sigma \approx \bar{U}_0/\sigma$.

U_t/σ	$\bar{e}$	$\bar{U}_0/\sigma$
0.0	0.798	0.798
0.2	0.6904	0.8904
0.4	0.5617	0.9617
0.6	0.4601	1.0601
0.8	0.3674	1.1674
1.0	0.2874	1.2874
1.2	0.2193	1.4193
1.4	0.1627	0.5627
1.6	0.1172	1.7172
1.8	0.0818	1.8818
2.3	0.0551	2.0551
2.5	0.0175	2.5175

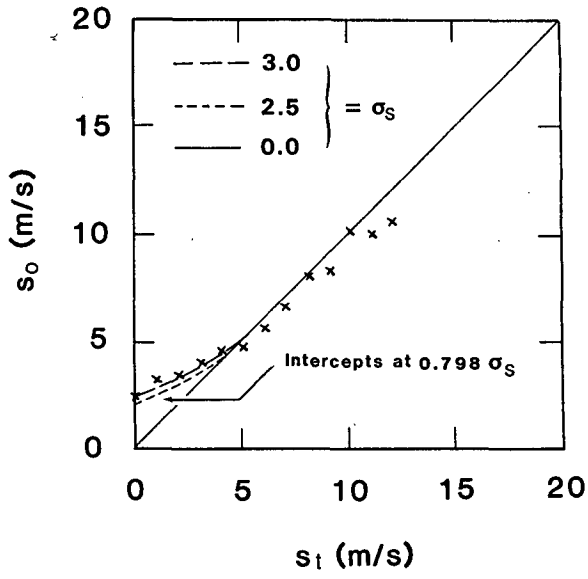

FIG. 1. Predicted and observed relationships between U_0 and U_t. The curves are from (5) with σ = 0.0, 2.5, and 3.0. The crosses are Gulf of Mexico observations for June through August 1979. Wind speeds from NOAA data buoys are used to represent U_t and speeds estimated from nearby ships are used for U_0. The minimum number of observations for each data point is 48. The uncertainty in the plotted points is $\pm\sigma/(n-1)^{1/2}$ or about $\pm$0.5 m s^{-1} for σ = 3.

3. Implications for cloud versus ship comparisons

The ratio of the speeds reported by cooperative merchant ships to the speeds of nearly colocated clouds tracked on sequences of images from the GOES satellite over the Indian Ocean for the period May–July 1979 are shown in Fig. 2. This figure arose in context of reducing the cloud motions to equivalent low-level wind speeds (Wylie and Hinton, 1984). The figure shows that ship reported winds are faster than cloud motions when the winds are light. This is not expected, since boundary layer friction implies that winds should usually decrease as one approaches the surface. Similar effects probably occur when comparing geostrophic winds and ship observations, as will be mentioned below.

Using (7), one can calculate the roughness height Z_0 from the drag coefficient $C_d(Z)$ for U_z, the wind at height Z, under neutral stratification for heights up to 100 or 200 m (Ch. 6, Part III, Fleagle and Businger, 1980). Von Karman's constant k is about 0.4.

$$C_d(Z) = k^2[\ln(Z/Z_0)]^{-2}. \quad (7)$$

From several candidate expressions, we adopted (8) from the work of Wu (1980) for the drag coefficient at 10 m.

$$C_d(10) = (0.8 + 0.065 \times U_{10})10^{-3}. \quad (8)$$

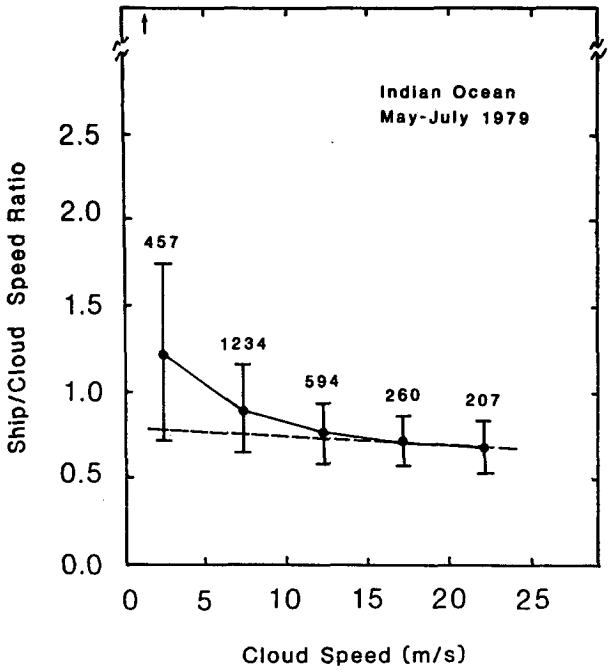

FIG. 2. Speed ratios in the Indian Ocean for May–July 1979. Points connected by the solid line segments are observations binned by cloud motion speed. The number of observations is shown over each pont. The standard deviations of the observed ratios are shown by the "error bars." The dashed curve represents the theoretically expected speed ratio based on (7)–(10). This is also shown in Table 3 as $U_{19.5}/U_{1000}$.

Using the logarithmic law (9) and Z_0 values from Table 2, one can calculate the expected values of $U_{19.5}$ and $U_{10}/U_{19.5}$ displayed in Table 3;

$$U_z/U_* = k^{-1}[\ln(Z/Z_0) + \mu]. \quad (9)$$

In (9), U_* is the "friction velocity" or $kZ\partial u/\partial Z$, and the function μ represents the effects of atmospheric stratification. For simplicity, assume μ is zero. The stratification in the observed data is moderate and does not materially affect our conclusions. The height 19.5 m corresponds to the equivalent height for the merchant ship observations.

TABLE 2. Roughness height for various wind speeds using the drag coefficient given by Wu (1980).

U_{10} (m s^{-1})	$C_d(10)$ ($\times 10^{-3}$)	z_0 ($\times 10^{-5}$ m)
1	0.87	1.2
2	0.93	2.0
3	0.99	3.1
4	1.06	4.6
5	1.12	6.6
6	1.19	9.2
10	1.45	27.4
15	1.77	75.3
30	2.75	480.0

TABLE 3. Relationships of U_{10}, $U_{19.5}$, and U_{1000} for neutral stratification.

U_{10}	$U_{10}/U_{19.5}$	$U_{19.5}$	$U_{19.5}/U_{1000}$
~0	0.953	~0	0.814
3	0.945	3.16	0.806
5	0.947	5.28	0.796
10	0.940	10.64	0.775
15	0.934	16.06	0.756
30	0.920	32.60	0.714

At height H, at the top of the Ekman-Taylor layer, somewhat above 100–200 m, the wind is expected to be geostrophic. In this case, it has been shown (Fleagle and Businger, 1980) that

$$U_g = k^{-1}[(\ln H/Z_0 - A)^2 + B^2]^{1/2}, \quad H = U_*/f. \quad (10)$$

Brown (1982) suggests that the height scale, U_*/f, which is supposed to represent the boundary layer height in Ekman theory, ought to be replaced by the actual boundary layer height. This is especially appealing at low latitudes to avoid the geostrophic catastrophe induced in (10) as f approaches zero. We have, therefore, replaced U_*/f by an approximate height scale as suggested.

Low-level clouds are found near the top of the planetary boundary layer. Typically, their motions represent winds near 900 mb or ~1000 m (Hasler *et al.*, 1979).[1] Consequently, if the similarity parameters A and B in (10) are assigned values, we can calculate $U_{19.5}/U_H$ from (9) and (10). These values are also shown in Table 3 for $A = 1$, $B = 2$, and $H = 1000$ (See Fig. 1, Brown, 1982). It is easily shown from (9) that $U_{19.5}/U_H$ is not very sensitive to H so that the assumption $H = 1000$ is adequate. For example, if H were 600 m the speed ratio would change only 3% for speeds around 5 m s^{-1}. Nor is the speed ratio very sensitive to the specific drag coefficient formulation as one might suppose. Due to the logarithmic expressions in (7) and (9) even a (very extreme) factor of two change in C_d would change $U_{19.5}/U_{1000}$ only by 8%. The $U_{19.5}/U_{1000}$ entries from Table 3 are also plotted in Fig. 2 as the dashed curve.

The disturbing feature of Fig. 2 is the lack of justification for observed ship/cloud speed ratios in excess of one. (Nor can this effect be attributed to the effects of stability.) A similar situation confronted Hasse and Wagner (1971), who compared surface winds and geostrophic winds.

We shall now show how Fig. 2 may be explained by means of Fig. 3. Curve A represents the speed ratio one would expect to observe if the ratio of true surface

[1] Further data can be found in Hubert and Thomasell, 1979. This report shows that 900 mb corresponds to the average "level of best fit" to nearby radiosondes. Over 70% of the time low-level clouds reflect motions between 1000 mb and 810 mb.

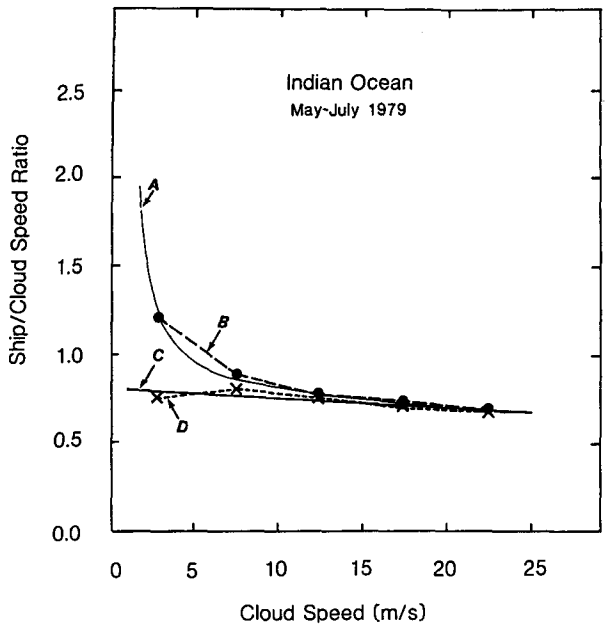

FIG. 3. Expected and observed speed ratios. Curve A shows expected ratios of ship-observed speed to cloud level speed when ship speeds contain the uncorrected $\sigma\bar{e}$ error. Curve B illustrates the experimentally observed ratios using uncorrected ship data. The data shown are the same as in Fig. 2. Curve C portrays the speed ratios from boundary layer theory alone. Therefore, it represents the ratios one would expect with perfect data. Curve D is the experimentally derived relationship if the mean ship speeds are corrected by subtracting $\sigma\bar{e}$. It is obtained from the same data set as curve B. Curves A and D correspond to $\sigma = 3$.

speed to cloud level speed were given correctly by boundary layer theory alone, but the measured surface speed exceeded the true surface speed by the statistical error $\sigma\bar{e}$. Curve B, consisting of dots joined by dashes, shows the mean observed ratios (as in Fig. 2). That is, curve B is plotted from binned means of ship-observed winds over matched cloud motion speeds. The ship observations are hypothesized to incorporate the error $\sigma\bar{e}$. Consequently, we expect Curve B to agree with curve A.

Curve C illustrates ratios of ship-observed speeds to cloud level speeds predicted by boundary layer theory. These are the ratios we would expect if ship observations were error free or if actual observations were modified by a valid correction. Curve D, crosses joined by the dotted line, displays ratios computed from the observed ship speeds with the correction $\sigma\bar{e}$ subtracted. Consequently, we expect curve D to agree with curve C.

The good agreement of curve A with B and of curve C with D suggest that $\sigma\bar{e}$ is an appropriate correction and σ is about 3, as previously noted.

4. Conclusions

We conclude that ship wind data need to be corrected as shown by (6), using $\sigma \approx 2.5$–3.0 m s^{-1}. Comparisons of cloud level winds to surface winds might be better if based on the boundary layer theory (curve A in Fig. 3), rather than observed ship/cloud speed ratios derived from the averaged uncorrected ship data (curve B in Fig. 3). However, after subtraction of the appropriate $\sigma\bar{e}$ (Table 1) from the ship speed, one could obtain "observed" ratios nearly identical to those from theory shown by curve C in Fig. 3. We further suggest that the results of Hasse and Wagner (1971) may be explained in the same way we have explained the ship/cloud speed ratios. It follows that improved relations can be derived between geostrophic, or cloud motion, winds and surface winds. These relations will give better surface speed estimates, especially at low speeds when cloud motions or geostrophic winds are used as proxy data in lieu of surface measurements.

Acknowledgments. This work was sponsored by Grant ATM-81 19895 from the National Science Foundation and Contract NAG5-301 from the National Aeronautics and Space Administration.

REFERENCES

Brown, R. A., 1982: On two-layer models and the similarity functions for the PBL. *Bound. Layer Meteor.*, **24,** 451–463.

Fleagle, R. G., and J. A. Businger, 1980: *An Introduction to Atmospheric Physics,* 2nd Ed., Academic Press, 432 pp.

Hasler, A. F., W. C. Skillman, W. E. Shenk and J. Steranaka, 1979: *In situ* aircraft verification of the quality of satellite cloud winds over oceanic regions. *J. Appl. Meteor.*, **18,** 1481–1489.

Hasse, L., and V. Wagner, 1971: On the relationship between geostrophic and surface wind at sea. *Mon. Wea. Rev.* **99,** 255–260.

Hubert, L. F., and A. Thomasell, 1979: Error characteristics of satellite-derived winds. NOAA Tech. Rep. NESS 79, 35 pp.

WMO, 1970: The Beaufort scale of wind force. Rep. No. 3, Reports on Marine Science Affairs, World Meteorological Organization, Geneva, Switzerland.

Wu, J., 1980: Wind-stress coefficients over sea surface near neutral conditions—A revisit. *J. Phys. Oceanogr.*, **10,** 717–740.

Wylie, D. P., and B. B. Hinton, 1982: A comparison of cloud motion and ship wind observations over the Indian Ocean for the year of FGGE. *Bound. Layer Meteor.*, **23,** 197–208.

——, and ——, 1984: Factors affecting boundary layer wind shear over the Indian Ocean during FGGE. *Bound. Layer Meteor.*, **28,** 391–407.